

Developing silicon carbide for quantum spintronics


Cite as: Appl. Phys. Lett. **116**, 190501 (2020); <https://doi.org/10.1063/5.0004454>

Submitted: 11 February 2020 • Accepted: 06 April 2020 • Published Online: 11 May 2020

 Nguyen T. Son,  Christopher P. Anderson,  Alexandre Bourassa, et al.

COLLECTIONS

 This paper was selected as Featured

 This paper was selected as Scilight



View Online



Export Citation



CrossMark

ARTICLES YOU MAY BE INTERESTED IN

[Material platforms for defect qubits and single-photon emitters](#)

Applied Physics Reviews **7**, 031308 (2020); <https://doi.org/10.1063/5.0006075>

[Development of microLED](#)

Applied Physics Letters **116**, 100502 (2020); <https://doi.org/10.1063/1.5145201>

[Quantum dot arrays in silicon and germanium](#)

Applied Physics Letters **116**, 080501 (2020); <https://doi.org/10.1063/5.0002013>

Lock-in Amplifiers
up to 600 MHz



Zurich
Instruments



Developing silicon carbide for quantum spintronics



Cite as: Appl. Phys. Lett. **116**, 190501 (2020); doi: 10.1063/5.0004454

Submitted: 11 February 2020 · Accepted: 6 April 2020 ·

Published Online: 11 May 2020



Nguyen T. Son,^{1,a)} Christopher P. Anderson,^{2,3} Alexandre Bourassa,² Kevin C. Miao,² Charles Babin,⁴ Matthias Widmann,⁴ Matthias Niethammer,⁴ Jawad Ul Hassan,¹ Naoya Morioka,⁴ Ivan G. Ivanov,¹ Florian Kaiser,⁴ Joerg Wrachtrup,^{4,5} and David D. Awschalom^{2,3,6}

AFFILIATIONS

¹Department of Physics, Chemistry and Biology, Linköping University, SE-58183 Linköping, Sweden

²Pritzker School of Molecular Engineering, University of Chicago, Chicago, Illinois 60637, USA

³Department of Physics, University of Chicago, Chicago, Illinois 60637, USA

⁴3rd Institute of Physics, University of Stuttgart and Institute for Quantum Science and Technology IQST, 70569 Stuttgart, Germany

⁵Max Planck Institute for Solid State Research, 70569 Stuttgart, Germany

⁶Center for Molecular Engineering and Materials Science Division, Argonne National Laboratory, Lemont, Illinois 60439, USA

^{a)} Author to whom correspondence should be addressed: tien.son.nguyen@liu.se

ABSTRACT

In current long-distance communications, classical information carried by large numbers of particles is intrinsically robust to some transmission losses but can, therefore, be eavesdropped without notice. On the other hand, quantum communications can provide provable privacy and could make use of entanglement swapping via quantum repeaters to mitigate transmission losses. To this end, considerable effort has been spent over the last few decades toward developing quantum repeaters that combine long-lived quantum memories with a source of indistinguishable single photons. Multiple candidate optical spin qubits in the solid state, including quantum dots, rare-earth ions, and color centers in diamond and silicon carbide (SiC), have been developed. In this perspective, we give a brief overview on recent advances in developing optically active spin qubits in SiC and discuss challenges in applications for quantum repeaters and possible solutions. In view of the development of different material platforms, the perspective of SiC spin qubits in scalable quantum networks is discussed.

© 2020 Author(s). All article content, except where otherwise noted, is licensed under a Creative Commons Attribution (CC BY) license (<http://creativecommons.org/licenses/by/4.0/>). <https://doi.org/10.1063/5.0004454>

In the quest for computational power, technological development in downsizing elements of semiconductor devices, such as transistors, is approaching the quantum regime, where the information processing must be performed on systems whose behavior is governed by the laws of quantum mechanics. Such quantum systems play a role as basic units of information, often called quantum bits (qubits). Many quantum systems from different material platforms, such as superconducting circuits, trapped ions, neutral atoms, and solid-state spins, are currently being developed.¹ With specific properties and differing levels of control in realization, initialization, manipulation, and readout, each quantum system has distinct advantages for quantum technologies.

Solid-state qubits, including quantum dots (QDs) and color centers in crystals, are promising for quantum information processing and nanoscale sensing.¹ Single photon emitters from III–V semiconductor QDs are attractive for applications in quantum key distribution (QKD), where there has been noticeable progress in tuning the

emission of self-assembled QDs to the telecom wavelengths.² A long-distance (120 km) QKD over a fiber network has been demonstrated although the rates of raw and secure keys are still one to two orders of magnitude slower than those for attenuated-laser QKD.³ A QD involving a trapped electron or hole can act as an optical spin qubit that combines single photon emission and a correlated spin qubit.⁴ Quantum entanglement between distant qubits—an important feature for quantum networks—has been demonstrated using these systems.⁵ However, short spin coherence and quantum storage times caused by magnetic noise from the nuclear spin bath of III–V semiconductors remain a major challenge for QDs.⁴ These short coherences limit the distances that photons can travel before the correlated quantum memory decoheres. Additionally, the wide variation of photoemission properties among self-assembled QDs caused by their random nature is also an issue in the fabrication of QDs emitting indistinguishable single photons.

Point defects in wide-bandgap semiconductors introduce deep levels in the bandgap and can have a non-zero spin.^{6–8} Many defects have both ground and excited states within the bandgap and, hence, are color centers with associated absorption and emission from transitions between these states. At low temperatures, these orbital states resolve and form a spin-photon interface. Spin qubit density can be controlled precisely in defect-free substrates, allowing the observation of single emitters. In crystal hosts with low natural abundance of non-zero nuclear spins, such as diamond, silicon carbide (SiC), and II–VI compounds, spins associated with color centers can have long coherence times.⁹ Optically addressable spins with a long coherence time even at ambient conditions, the availability of nuclear spins for quantum memories, and high-fidelity spin-to-photon interfaces are distinct advantages of color centers for applications in quantum information processing and quantum sensing.^{7,8}

The nitrogen-vacancy (NV) center in diamond, i.e., a complex between a substitutional nitrogen and a nearest lattice vacancy, is the most-studied system among solid-state spins. Its recent major advances include the demonstration of nuclear magnetic resonance spectroscopy at the scale of single cells using an ensemble of NV centers,¹⁰ atomic-scale imaging of a 27-nuclear-spin cluster using a single NV center,¹¹ realization of a ten-qubit register consisting of a NV center and nine nuclear spins with quantum memory up to one minute,¹² and high-fidelity (92%) entanglement of photons from two NV centers separated by ~ 1.3 km, establishing protocols for quantum repeaters.¹³ For extension to existing telecommunication-band fiber networks, recent experiments have shown entanglement-preserving quantum frequency conversion (QFC) of single NV photons at 637 nm into telecom frequencies with an efficiency of 17%.¹⁴ However, down-frequency conversion, which more than doubles the wavelength, comes at the cost of extra-noise photons due to spontaneous scattering processes of the strong laser pump with a wavelength shorter than that of the converted signal.¹⁵

Several group-IV related color centers in diamond, e.g., the silicon-vacancy (SiV),¹⁶ germanium-vacancy (GeV),¹⁷ and tin-vacancy (SnV),¹⁸ have recently emerged as promising spin qubits due to their favorable optical properties with a high Debye–Waller (DW) factor ($\sim 70\%$ of emission at the zero phonon line (ZPL) for the SiV and GeV centers) and narrow optical linewidths. These centers benefit from crystallographic inversion symmetry that prevents a first-order Stark shift, suppressing spectral diffusion, but have the caveat that relevant spin coherence times may require relatively low temperatures down to the mK range.^{16,17} With ZPLs at visible wavelengths (~ 737 nm for SiV,¹⁶ ~ 602 nm for GeV,¹⁷ and ~ 619 – 620 nm for the SnV center¹⁸), these centers will also have noise photons in QFC to telecom bands similar to the NV center. Alternative spin-active color centers beyond diamond with more favorable intrinsic properties for efficient long-distance entanglement have been an active area of research.⁶

Silicon carbide is a wide-bandgap semiconductor, which can exist in many polytypes with the hexagonal 4H–SiC (bandgap: 3.23 eV) and 6H–SiC (3.0 eV) and cubic 3C–SiC (2.36 eV) polytypes being the most common. This compound material is known to be superior for energy-efficient power electronics and is the only wide-bandgap semiconductor with the established large-scale industrial production methods, controlled doping, well-developed integrated circuit processing, and high-quality nanofabrication. As both are wide-bandgap materials, SiC and diamond share most of the favorable properties for

quantum technology, with many optically active spin qubits developed with a long coherence time and room temperature operation.^{6,9,19–21} In addition, in SiC, the defect spins can have even longer coherence times compared to diamond. This is due to several factors: the smaller gyromagnetic ratio of ²⁹Si nuclei, the larger bond length in the SiC lattice, the suppression of the heteronuclear spin pair flip-flop process,²² the decoupling of ²⁹Si and ¹³C paramagnetic nuclear spin baths under a moderate magnetic field (~ 30 mT or above), the dilution of homonuclear spin pairs, and the absence of strongly coupled, nearest-neighbor spin pairs.²¹ Furthermore, certain defects in SiC benefit from clock-like transitions that protect quantum coherence.²³ In principle, SiC can combine the best of diamond's properties and the benefits of industrial wafer-scale materials with well-controlled n- and p-type doping, standard CMOS processing, mature nanofabrication techniques, and high-quality micro electromechanical systems (MEMS)²⁴ technology.

The most-studied color centers in SiC include the neutral divacancy ($V_C V_{Si}^0$), i.e., an uncharged complex consisting of a C vacancy (V_C) and a nearest Si vacancy (V_{Si}), and the negative Si vacancy (V_{Si}^-). Recently, isolated single neutral divacancy¹⁹ and negative Si vacancy²⁰ emitters have been realized, showing their optically addressable spins with millisecond coherence times.

In 4H–SiC, two types of V_{Si}^- centers are observed on inequivalent lattice sites, leading to a ZPL emission at 861.6 nm for the V1 center and 916.5 nm for the V2 center.²⁵ Similarly, in 6H–SiC, three ZPL emission lines are observed at 864.7 nm, 886.3 nm, and 907.1 nm for the V1, V2, and V3 centers, respectively.²⁵ Due to short C dangling bonds, V_{Si}^- keeps the C_{3v} symmetry and has a high-spin ground state 4A_2 with an electron spin of $S = 3/2$ and the lowest excited state 4A_2 . Optical transitions $^4A_2 \rightarrow ^4A_2$ of the V1–V3 lines have the optical dipole moment oriented along the *c*-axis ($E||c$).²⁶ Despite the lack of inversion symmetry, the optical transition of the V_{Si}^- center and, hence, its linewidth is expected to be less sensitive to charge variation in local environments due to similar dipole moments in the ground and excited states.²⁷

The efficient optical initialization of the V1 electron spin state (97.5%) helps to reach a high optical contrast of spin readout by optically detected magnetic resonance (ODMR) (97%) using resonant excitation.^{28,29} Optical transitions with narrow linewidths of ~ 60 MHz, which are only twice the lifetime limit, have been reported for V1 in 4H–SiC with a doping level of $\sim 6 \times 10^{13}$ cm⁻³.²⁹ A long spin coherence time exceeding 20 ms in commercial 4H–SiC wafers has been reported for the V2 center using dynamical decoupling in combination with spin-locking.³⁰ Efficient spin polarization and spin-to-charge conversion enable electrical readout of V_{Si}^- electron spins at room temperature using photocurrent detected magnetic resonance (PDMR).³¹ For QFC of V_{Si}^- emission to the telecom C-band (~ 1550 nm), the laser pump should be at wavelengths far longer than 1550 nm, and therefore, no photonic excess noise at the converted wavelength should be expected.³²

The $V_C V_{Si}^0$ center in 4H–SiC emits light at near-telecom wavelengths (at 1078–1132 nm for ZPLs of its four configurations⁹ and at 1037–1047 nm for other ZPLs corresponding to $V_C V_{Si}^0$ located near stacking faults³³). The Hahn-echo spin coherence time of the neutral divacancy in a commercial 4H–SiC wafer with natural isotope abundance reaches the millisecond range.^{21,34} The neutral divacancy in 4H–SiC has a similar electronic structure as the NV center in diamond

but with a lower degree of intrinsic spin-mixing in the 3E excited state.³⁵ This is expected to result in a slower spin flip rate, which can increase the number of emitted photons before destroying the quantum state. This is required for achieving high-fidelity single-shot readout of spin states, a necessary component for nodes in a quantum network. This reduced spin mixing and the high level of ground state polarization help to reach a 98% ODMR contrast under resonant excitation.³⁴ Quantum entanglement of a macroscopic divacancy spin ensemble in a commercial SiC wafer at ambient conditions has recently been demonstrated with nuclear spin quantum memories, presenting an important step toward practical quantum technology.³⁶ The low fiber loss in this spectral range (~ 0.7 dB/km for $V_C V_{Si}^0$ vs 8 dB/km for the NV center in diamond) will dramatically increase distances possible in quantum communication protocols. Further, QFC of the $V_C V_{Si}^0$ emission into the optimized telecom C-band (with a fiber loss of ~ 0.25 dB/km) is expected without adding extra-noise photons.³²

Transition metal (TM) impurities in SiC are often color and paramagnetic centers as well.³⁷ The exciton-bound to neutral titanium, with a singlet ground state ($S=0$) and a triplet excited state ($S=1$),³⁸ is of interest for utilizing nuclear spin memories since hyperfine interaction can be switched off in the ground state ($S=0$) after polarizing nuclear spins via the excited state spin. Other identified TM impurities in SiC emit in the near-infrared region, such as neutral niobium ($Nb_{Si} V_C^0$),^{39,40} neutral chromium (Cr^{4+}),⁴¹ positive molybdenum (Mo^{5+}),^{42,43} and positive tungsten (W^{5+}),⁴⁴ and in the telecom

O-band, such as neutral vanadium (V^{4+}).^{45,46} Another impurity-related color center in SiC, which emits light at the near-telecom band, is the nitrogen-Si vacancy center ($N_C V_{Si}$), i.e., the complex between N at a C site and a nearest neighbor Si vacancy.^{47,48}

Favorable optical and spin properties for quantum communication have already been shown for Cr^{4+} ,^{49,50} Mo^{5+} ,⁴³ and the V^{4+} center.^{45,46} Recent studies show large DW factors for V^{4+} (22% and 39% for $V^{4+}(h)$ and $V^{4+}(k)$ at the hexagonal and cubic lattice sites, respectively^{45,46}) and for Cr^{4+} (73%).⁴⁹ Since TMs are not common impurities in SiC, their concentration in the as-grown materials is negligible, allowing for intentional doping or localized implantation to a low level possible for observation of single emitters. Recently, single neutral V^{46} and $N_C V_{Si}$ ^{51,52} emitters have been realized in 4H-SiC by V and N implantation, respectively. Another advantage of impurity-related color centers is the availability of intrinsic nuclear spins to the impurity, which can be used as quantum memories. A list of potential spin-active color centers in SiC and their properties is given in Table I.

Extraction of photons from SiC defects correlated with the spin state is a common problem in the field. Spin-active color centers in SiC with efficient optical initialization of spin, such as V_{Si}^- , may not have bright fluorescence. The typical reported count rate of single Si-vacancy V1 and V2 emitters is 3–5 kcts/s and can be increased to 30–40 kcts/s using solid immersion lens (SILs) to increase collection efficiency.²⁰ The main reason for weak photoluminescence (PL) emissions of V1 and V2 is due to efficient non-radiative recombination via the intersystem crossing (ISC).^{56,57} With weaker ISC of the $S=1$

TABLE I. Potential spin-active color centers in SiC.

Defects	Polytype	ZPL (nm)	DW (%)	S	ZFS (GHz)	References
V_{Si}^-	4H	861–916	8–9	3/2	0.0025–0.035	26,53
	6H	864–907		3/2	0.0027–0.127	25,26
$V_C V_{Si}^0$	4H	1078–1132	5–10	1	1.22–1.34	9,23,34,54
	4H	1037–1047 ^a		1	1.35–1.37	9,33
	6H	1092–1139		1	1.21–1.36	55
	3C	1106		1	1.336	35
	4H	1176–1242		1	1.270–1.313	47,48
$N_C V_{Si}^-$	6H	~ 1240 – 1305 ^b	22–50	1	1.278–1.355	47
	3C	~ 1440 ^b		1	1.303	47
	4H	1278–1334		1/2		45,46
V^{4+}	6H	1308–1388	25–50	1/2		46
	4H	1042–1070		73	1	1.057–6.711
Cr^{4+}	6H	1043–1073	1		1	
	4H	1076		1/2		43
Mo^{5+}	6H	1121	1/2	1/2		42,43
	4H	822–896		1/2		39,40
$Nb_{Si} V_C^0$	6H	906–911	1/2	1/2		39,40
	4H	1170–1171		1/2		44
W^{5+}	6H	1237–1245	1/2	1/2		44
	4H	435–444		1 ^c	10.96–11.16	38
Ti	6H	419–445	1 ^c	1 ^c	10.70–14.93	38

^aDivacancy at stacking faults.

^bCalculated values.

^cIn the excited state.

system and lower mixing of the excited state 3E ,³⁵ single $V_C V_{Si}^0$ emitters have brighter emission (~ 40 – 50 kcts/s without SILs).

The broad emission spectrum of V1, V2, and $V_C V_{Si}^0$ centers, with only a small fraction of total photons being coherently emitted into the ZPL, further reduces the number of indistinguishable photons. This drastically impacts the probability of the two-photon interference events required to make a quantum communication channel between solid-state qubits. Coupling quantum emitters into small mode volume photonic cavities is an efficient way to concentrate the emission into the ZPL through the Purcell effect, enhancing the number of photons emitted at the same wavelength while also improving the efficiency of light collection. Such photonic enhancement would drastically improve entanglement rates in a quantum network and may also mitigate issues of low quantum efficiency from non-radiative pathways.⁵⁸ Providing such an improvement, while maintaining excellent optical properties, would certainly induce the transition from proof-of-concept demonstrations to relevant quantum information and communication applications at scale.

Recent studies of a Si vacancy ensemble embedded in a nano-beam photonic 4H-SiC crystal cavity have shown an enhancement of the ZPL of V1 and V1', which corresponds to the transition from the second excited state 4E (~ 4.5 meV above the lowest excited state 4A_2)²⁶ of the V1 center to its ground state 4A_2 , by a factor of 22 and 75, respectively.⁵⁹ An enhancement of emission from single V1 emitters in the nanophotonic cavity in 4H-SiC on insulator (SiCOI) by a factor of 120 compared to off-resonant emission has also been achieved in a recent study.⁶⁰ Similarly, the integration of single $V_C V_{Si}^0$ emitters into a nanophotonic crystal cavity has been realized, showing Purcell enhancement by a factor of ~ 50 and coherent spin control of the ground state.⁶¹ This nanophotonic integration results in an enhanced count rate of 460 kcts/s and an increase in the DW factor from $\sim 5\%$ to 70%–75%.⁶¹ This improvement in the DW factor is expected to significantly increase (by a factor of ~ 200) the entanglement rates between two individual $V_C V_{Si}^0$ emitters. This system also achieved an improvement by a factor of 2.5–3 in off-resonant collection efficiency and a threefold decrease in the lifetime, which corresponds to triple the emission events before a spin flip.⁶¹

A QFC of near-infrared light into the telecommunication band with near-unity internal photon conversion efficiency using microring resonators fabricated on a SiC nanophotonic platform has been demonstrated, showing that applications for both the enhancement of quantum emitters and down-frequency conversion to the telecom frequencies can be implemented with a 4H-SiCOI architecture on a single photonic chip.⁶⁰ Matured and recently developing SiC nanophotonic fabrication techniques^{59–62} provide a clear path for enhancing defect properties and boosting communication rates on a solid-state platform.

Resonant excitation helps to achieve high contrast in ODMR detection of single Si vacancies^{28,29} and divacancies.^{34,35} However, quenching of PL emission is a common problem under resonant excitation. For the neutral divacancies, the decay of the PL emission is observed under resonant excitation or off-resonant excitation with photon energies lower than ~ 1.28 eV.^{63,64} Repumping with a higher photon energy can recover the negative charge state of the Si vacancy^{29,57} and the neutral charge state of the divacancy.^{34,35,63} It is noticed that if the material is n-type, even with a low doping level of $3 \times 10^{14} \text{ cm}^{-3}$, repumping can recover the negative charge state of V_{Si} , but the V_{Si}^- emission still decays exponentially with a timescale of

10 ms, resulting in photobleaching of single emitters.⁵⁷ Charge stability and blinking for emitters in solids are general problems that require a careful study.

It has been shown recently that the charge state, brightness, and photostability of single $V_C V_{Si}^0$ and V_{Si}^- emitters integrated in the depleted region of a vertical semiconductor p–i–n diode can also be efficiently regulated by the applied electric field in combination with properly chosen optical excitation.^{34,65} A large tuning range of the quasi Fermi level in the i-layer and optical excitation allow for switching off and on single emitters, modulating their PL emission in time with the gate voltage, creating an electrically gated single-photon source.³⁴ More specifically, the field enables a reduction in the random recapturing of photoexcited free carriers. This approach allows for the ability to maintain the stability of the charge state and PL emission of the quantum emitters. Moreover, such a device can be conveniently used for Stark tuning, which is up to a few hundred GHz for the Si vacancy⁶⁶ and divacancy³⁴ centers, enabling temporal photon shaping by dynamically tuning the spectral emission as well as the creation of many spectrally multiplexed entanglement channels. Additionally, Stark tuning can be used for coupling single emitters to cavity modes and for tuning remote spin defects into mutual resonance to achieve long-distance entanglement. Alternatively, combining pure materials with a doping level of residual impurities to below the 10^{14} cm^{-3} range with a careful choice of excitation, stable charge states and photostability can also be achieved for single emitters of the Si vacancy²⁹ and divacancy³⁵ centers.

The incorporation of some impurities and introduction of certain intrinsic defects during material fabrication are common for all solids, especially for crystal semiconductors grown at high temperatures such as SiC. The fluctuating charge and spin of nearby defects cause spin decoherence of the optically active qubit. Moreover, their fluctuation influences the optical fine structure of quantum emitters. Under optical excitation, charge transfer from capturing and ionizing processes of nearby defects creates fluctuating electrical environments, which cause random jumps in the wavelength of the ZPL of single emitters (known as spectral diffusion), leading to inhomogeneous line broadening. Spectral diffusion has been a notoriously difficult challenge for quantum emitters in solids including diamond, SiC, and quantum dots, which reduces the fidelity of the entanglement-producing two-photon interference.

For suppressing spectral diffusion of quantum emitters from centers with no crystallographic inversion symmetry such as V_{Si}^- and $V_C V_{Si}^0$, one strategy is to reduce electric field noise by either depleting the local charge environment of defects or reducing the concentration of impurities and electron traps in the host material. The former approach has been demonstrated for single $V_C V_{Si}^0$ emitters in 4H-SiC p–i–n diodes with a N concentration of $\sim 1 \times 10^{15} \text{ cm}^{-3}$ in the i-layer. Combining a proper excitation with a high reverse bias, charge carriers can be efficiently depleted and very stable emission with a narrow optical linewidth of ~ 20 MHz (approximately twice the lifetime limit), which corresponds to an improvement in the linewidth of a factor of more than 50, has been achieved [Figs. 1(a)–1(d)].³⁴ The obtained results demonstrate that the charge depletion in diode structures is a very efficient way to stabilize the emission and to suppress the spectral diffusion of quantum emitters even in impure materials.

The latter approach, i.e., to reduce the overall density of impurities and intrinsic defects in the material, can improve the spectral stability of

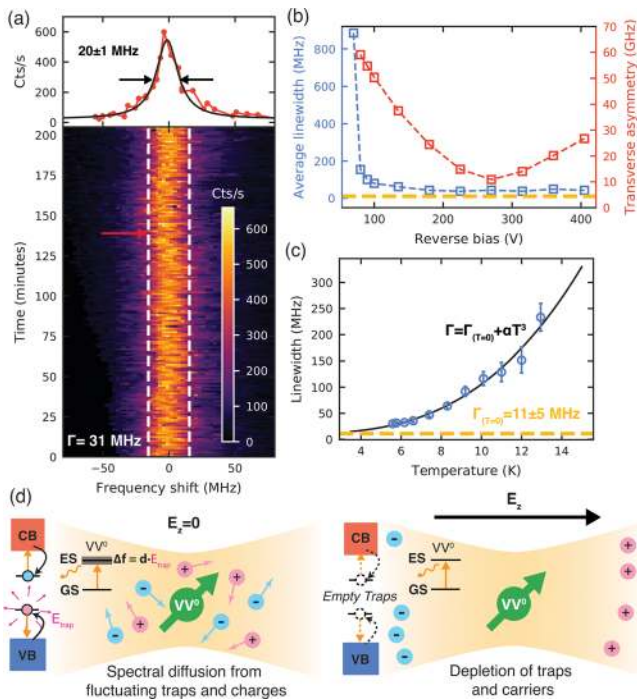


FIG. 1. Optical linewidth narrowing by tuning the electrical environment of a solid-state emitter. (a) Bottom shows that optical frequency is stable over many hours. Top shows a single line scan (at the red arrow) with a linewidth of 20 MHz. (b) shows (in blue) the linewidth narrowing of the optical line and (in red) a lowering of the transverse asymmetry. (c) shows that a lower temperature combined with fewer instrumental errors (estimated around 5 MHz) could have allowed for the measurement of the lifetime-limited line of around 11 MHz (yellow line). (d) Model for the effect of charge depletion on spectral diffusion in the illuminated volume (yellow). To the left of each diagram is a schematic band diagram with the relevant transitions. CB, conduction band; VB, valence band; GS, ground state; ES, excited state. Data in (a) and (b) were obtained at $T = 5$ K. Reproduced with permission from Anderson *et al.*, *Science* **366**, 1225 (2019). Copyright 2019 AAAS and Copyright Clearance Center.

emitters. Moreover, the presence of paramagnetic impurities can have an impact on the spin coherence. This may be especially important in isotopically purified materials since even at low concentrations, their relatively large dipole moment can contribute to unwanted magnetic noise. In high-purity 4H-SiC layers with concentrations of N, B, and the C vacancy in the 10^{13} cm^{-3} range, very stable PL of single V_{Si}^- emitters with a narrow optical linewidth of ~ 60 MHz has been observed.²⁹ Stable PL and small residual spectral diffusion of single V_{Si}^- emitters in pure 4H-SiC allow controlling the emission of indistinguishable and distinguishable photons and to demonstrate two-photon interference with contrast close to 90%.⁶⁷ Judging from the observed results, it is expected that a combination of charge depletion with ultrapure materials and annealing for removal of other radiation-induced defects will enable further linewidth narrowing of single V_{Si}^- and $V_{\text{C}}V_{\text{Si}}^0$ emitters to approach their natural linewidths.

Deterministic single-shot readout of individual electron spins is known to be a difficult challenge and has not yet been demonstrated for color centers in SiC. Readout is usually performed using spin-selective optical excitation, followed by detection of a few photons

emitted from the addressed transition.⁶⁸ Neutral divacancies show high count rates,^{34,35} such that deterministic electron spin single-shot readout seems to be feasible, potentially utilizing additional photonic crystal cavities for further boosting emission rates and photon collection efficiency.⁶¹

For single V_{Si}^- emitters, direct single-shot readout will be difficult due to the absence of a highly cycling optical transition. Additionally, applicable Purcell enhancement with cavities is limited since the resulting optical line broadening should not exceed the intrinsic small line splitting of about 1 GHz.²⁹ As shown in Fig. 2, a possible solution to this issue is using nearby nuclear spins as ancilla qubits. After completion of the quantum protocol on the electron spin, a nearby ^{29}Si nuclear spin is entangled with the electron spin. High-fidelity readout is then obtained by repeatedly performing electron-spin optical readout, initialization, and subsequent (classical) copying of the nuclear spin information onto the electron spin. We note that coherent coupling between a single V_{Si}^- center and a single nuclear spin has already been demonstrated²⁹ and that similar protocols are routinely used for room-temperature NV diamond experiments, achieving near-unity fidelities.⁶⁹⁻⁷¹

The development of solid-state qubits for quantum communication has been progressing faster than ever, and the improvement of their performance will continue with increasing pace. While current leading systems, such as the NV center in diamond, will be further refined, a combination of diverse quantum systems with complementary properties may lead to hybrid devices with optimized components and improved performance. With advantages regarding optical properties (especially in nanostructures), the recently emerged SiV, GeV, and SnV centers in diamond have become potential competitors in the field.

For the SiC platform, the spin coherence time of $V_{\text{C}}V_{\text{Si}}^0$ and V_{Si}^- will be further improved by material engineering and isotopic purification, as predicted.²¹ The stability of the charge state and PL emission of emitters are no longer an issue in pure materials. Small residual spectral diffusion achieved in pure materials or by charge depletion in a p-i-n diode will be further suppressed using diodes with purer i-layers. Successful single-shot readout of individual $V_{\text{C}}V_{\text{Si}}^0$ and V_{Si}^- emitters may soon be demonstrated. New spin qubits with better properties for long-distance quantum communications may be found among other impurity-related color centers in SiC. For example, the recently developed neutral V^{4+} center, with relatively bright

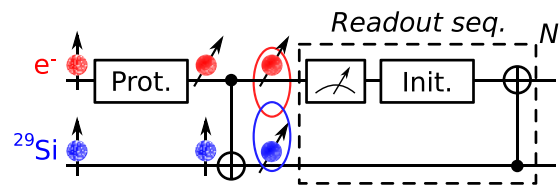


FIG. 2. Sketch of the basic protocol for achieving high-fidelity single-shot readout of V_{Si}^- electron spin using a nearby ^{29}Si nuclear spin. Both electron and nuclear spins are initialized, and then a quantum protocol is implemented using the electron spin. Thereafter, electron and nuclear spins are entangled using a CNOT gate. The final readout sequence is based on optical electron spin readout, electron spin initialization, and (classical) copying of the nuclear spin information onto the electron spin. The sequence is repeated multiple times N to improve the statistics and overall fidelity of the readout.

emission at the telecom O-band with a low fiber loss (~ 0.4 dB/km) and large DW factors, is particularly attractive.^{45,46}

In the next few years, successful QFCs of the Si vacancy and divacancy emission into telecom wavelengths using either periodically poled lithium niobate waveguides, as successfully performed for single QDs,³² or modal phase-matching in high-Q microring resonators⁶⁰ or nanophotonic cavities⁶² for second-harmonic generation, can be expected. Quantum repeaters using single emitters from the Si vacancy (with QFC into the telecom C-band), the neutral divacancy, and the neutral vanadium center in 4H-SiC and test experiments using such quantum repeaters for proof-of-principle “quantum links” via existing fiber networks may be demonstrated.

Challenges in the field are no longer purely scientific but have become a matter of combining device engineering with fundamental research, such as in material engineering and integrated photonic chips necessary for scaling quantum networks. With advantages of a wafer-scale CMOS-compatible material having established nanofabrication techniques, including SiCOI, well-controlled doping down to an ultrapure level, and hosting various spin-active color centers emitting light near and at the telecom wavelengths with favorable properties for applications in quantum repeaters, SiC has potential to take the lead in the development of scalable quantum networks.

Financial support from the Swedish Research Council for N.T.S. (No. VR 2016-04068) and I.G.I. (No. VR 2016-05362) and from the Swedish Energy Agency (No. 43611-1) for J.U.H. is acknowledged. N.T.S., J.U.H., and I.G.I. acknowledge funding by the EU H2020 Project QuanTELCO (No. 862721) and the Knut and Alice Wallenberg Foundation (KAW 2018.0071). J.W. acknowledges funding by the EU via projects QIA and SMel as well as the BMBF via Q.Link.X. C.A., A.B., K.C.M., and D.D.A. are supported by AFOSR Nos. FA9550-15-1-0029 and FA9550-19-1-0358, DARPA No. D18AC00015KK1932, and ONR No. N00014-17-1-3026.

The data that support the findings of this study are available from the corresponding author upon reasonable request.

REFERENCES

- T. D. Ladd, F. Jelezko, R. Laflamme, Y. Nakamura, C. Monroe, and J. L. O'Brien, *Nature* **464**, 45 (2010).
- S. L. Portalupi, M. Jeter, and P. Michler, *Semicond. Sci. Technol.* **34**, 053001 (2019).
- K. Takemoto, Y. Nambu, T. Miyazawa, Y. Sakuma, T. Yamamoto, S. Yorozu, and Y. Arakawa, *Sci. Rep.* **5**, 14383 (2015).
- R. Warburton, *Nat. Mater.* **12**, 483 (2013).
- A. Delteil, Z. Sun, W. Gao, E. Togan, S. Faelt, and A. Imamoglu, *Nat. Phys.* **12**, 218 (2016).
- J. R. Weber, W. F. Koehl, J. B. Varley, A. Janotti, B. B. Buckley, C. G. Van de Walle, and D. D. Awschalom, *Proc. Natl. Acad. Sci. U. S. A.* **107**, 8513 (2010).
- M. Atatüre, D. Englund, N. Vamivakas, S.-Y. Lee, and J. Wrachtrup, *Nat. Rev. Mater.* **3**, 38 (2018).
- D. D. Awschalom, R. Hanson, J. Wrachtrup, and B. B. Zhou, *Nat. Photon.* **12**, 516 (2018).
- W. F. Koehl, B. B. Buckley, F. J. Heremans, G. Calusine, and D. D. Awschalom, *Nature* **479**, 84 (2011).
- D. R. Glenn, D. B. Bucher, J. Lee, M. D. Lukin, H. Park, and R. L. Walsworth, *Nature* **555**, 351 (2018).
- M. H. Abobeih, J. Randall, C. E. Bradley, H. P. Bartling, M. A. Bakker, M. J. Degen, M. Markham, D. J. Twitchen, and T. H. Taminiau, *Nature* **576**, 411 (2019).
- C. E. Bradley, J. Randall, M. H. Abobeih, R. C. Berrevoets, M. J. Degen, M. A. Bakker, M. Markham, D. J. Twitchen, and T. H. Taminiau, *Phys. Rev. X* **9**, 031045 (2019).
- B. Hensen, H. Bernien, A. E. Dréau, A. Reiserer, N. Kalb, M. S. Blok, J. Ruitenberg, R. F. L. Vermeulen, R. N. Schouten, C. Abellán, W. Amaya, V. Pruneri, M. W. Mitchell, M. Markham, D. J. Twitchen, D. Elkouss, S. Wehner, T. H. Taminiau, and R. Hanson, *Nature* **526**, 682 (2015).
- A. Tchebotareva, S. L. N. Hermans, P. C. Humphreys, D. Voigt, P. J. Harmsma, L. K. Cheng, A. L. Verlaan, N. Dijkhuizen, W. de Jong, A. Dréau, and R. Hanson, *Phys. Rev. Lett.* **123**, 063601 (2019).
- J. S. Pelc, C. Langrock, Q. Zhang, and M. M. Fejer, *Opt. Lett.* **35**, 2804 (2010).
- D. D. Sukachev, A. Sipahigil, C. T. Nguyen, M. K. Bhaskar, R. E. Evans, F. Jelezko, and M. D. Lukin, *Phys. Rev. Lett.* **119**, 223602 (2017).
- M. K. Bhaskar, D. D. Sukachev, A. Sipahigil, R. E. Evans, M. J. Burek, C. T. Nguyen, L. J. Rogers, P. Siyushev, M. H. Metsch, H. Park, F. Jelezko, M. Loncar, and M. D. Lukin, *Phys. Rev. Lett.* **118**, 223603 (2017).
- M. E. Trusheim, B. Pingault, N. H. Wan, M. Gündoğan, L. De Santis, R. Debroux, D. Gangloff, C. Purser, K. C. Chen, M. Walsh *et al.*, *Phys. Rev. Lett.* **124**, 023602 (2020).
- D. J. Christle, A. L. Falk, P. Andrich, P. V. Klimov, J. U. Hassan, N. T. Son, E. Janzén, T. Ohshima, and D. D. Awschalom, *Nat. Mater.* **14**, 160 (2015).
- M. Widmann, S.-Y. Lee, T. Rendler, N. T. Son, H. Fedder, S. Paik, L.-P. Yang, N. Zhao, S. Yang, I. Booker, A. Denisenko, M. Jamali, S. A. Momenzadeh, I. Gerhardt, T. Ohshima, A. Gali, E. Janzén, and J. Wrachtrup, *Nat. Mater.* **14**, 164 (2015).
- H. Seo, A. L. Falk, P. V. Klimov, K. C. Miao, G. Galli, and D. D. Awschalom, *Nat. Commun.* **7**, 12935 (2016).
- L.-P. Yang, C. Burk, M. Widmann, S.-Y. Lee, J. Wrachtrup, and N. Zhao, *Phys. Rev. B* **90**, 241203(R) (2014).
- K. C. Miao, A. Bourassa, C. P. Anderson, S. J. Whiteley, A. L. Crook, S. L. Bayliss, G. Wolfowicz, G. Thiering, P. Udvardhelyi, V. Ivády, H. Abe, T. Ohshima, A. Gali, and D. D. Awschalom, *Sci. Adv.* **5**, eaay0527 (2019).
- S. J. Whiteley, G. Wolfowicz, C. P. Anderson, A. Bourassa, H. Ma, M. Ye, G. Koolstra, K. J. Satzinger, M. V. Holt, F. J. Heremans, A. N. Cleland, D. I. Schuster, G. Galli, and D. D. Awschalom, *Nat. Phys.* **15**, 490 (2019).
- E. Sörman, N. T. Son, W. M. Chen, O. Kordina, C. Hallin, and E. Janzén, *Phys. Rev. B* **61**, 2613 (2000).
- E. Janzén, A. Gali, P. Carlsson, A. Gällström, B. Magnusson, and N. T. Son, *Physica B* **404**, 4354 (2009).
- P. Udvardelyi, R. Nagy, F. Kaiser, S.-Y. Lee, J. Wrachtrup, and A. Gali, *Phys. Rev. Appl.* **11**, 044022 (2019).
- R. Nagy, M. Widmann, M. Niethammer, D. B. R. Dasari, I. Gerhardt, Ö. O. Soykal, M. Radulaski, T. Ohshima, J. Vučković, N. T. Son, I. G. Ivanov, S. E. Economou, C. Bonato, S.-Y. Lee, and J. Wrachtrup, *Phys. Rev. Appl.* **9**, 034022 (2018).
- R. Nagy, M. Niethammer, M. Widmann, Y.-C. Chen, P. Udvardhelyi, C. Bonato, J. Ul Hassan, R. Karhu, I. G. Ivanov, N. T. Son, J. R. Maze, T. Ohshima, Ö. O. Soykal, A. Gali, S.-Y. Lee, F. Kaiser, and J. Wrachtrup, *Nat. Commun.* **10**, 1954 (2019).
- D. Simin, H. Kraus, A. Sperlich, T. Ohshima, G. V. Astakhov, and V. Dyakonov, *Phys. Rev. B* **95**, 161201(R) (2017).
- M. Niethammer, M. Widmann, T. Rendler, N. Morioka, Y.-C. Chen, R. Stöhr, J. Ul Hassan, S. Onoda, T. Ohshima, S.-Y. Lee, A. Mukherjee, J. Isoya, N. T. Son, and J. Wrachtrup, *Nat. Commun.* **10**, 5569 (2019).
- J. S. Pelc, L. Yu, K. De Greve, P. L. McMahon, C. M. Natarajan, V. Esfandyarpour, S. Maier, C. Schneider, M. Kamp, S. Höfling, R. H. Hadfield, A. Forchel, Y. Yamamoto, and M. M. Fejer, *Opt. Express* **20**, 27510 (2012).
- V. Ivády, J. Davidsson, N. Deleghan, A. L. Falk, P. V. Klimov, S. J. Whiteley, S. O. Hruszkewycz, M. V. Holt, F. J. Heremans, N. T. Son, D. D. Awschalom, I. A. Abrikosov, and A. Gali, *Nat. Commun.* **10**, 5607 (2019).
- C. P. Anderson, A. Bourassa, K. C. Miao, G. Wolfowicz, P. J. Mintun, A. L. Crook, H. Abe, J. Ul Hassan, N. T. Son, T. Ohshima, and D. D. Awschalom, *Science* **366**, 1225 (2019).
- D. J. Christle, P. V. Klimov, C. F. de las Casas, K. Szász, V. Ivády, V. Jokubavicius, J. Ul Hassan, M. Syväjärvi, W. F. Koehl, T. Ohshima, N. T. Son, E. Janzén, A. Gali, and D. D. Awschalom, *Phys. Rev. X* **7**, 021046 (2017).

- ³⁶P. V. Klimov, A. L. Falk, D. J. Christle, V. V. Dobrovitski, and D. D. Awschalom, *Sci. Adv.* **1**, e1501015 (2015).
- ³⁷J. Baur, M. Kunzer, and J. Schneider, *Phys. Status Solidi A* **162**, 153 (1997).
- ³⁸K. M. Lee, L. S. Dang, and G. D. Watkins, *Phys. Rev. B* **32**, 2273 (1985).
- ³⁹N. T. Son, X. T. Trinh, A. Gällström, S. Leone, O. Kordina, E. Janzén, K. Szász, V. Ivády, and A. Gali, *J. Appl. Phys.* **112**, 083711 (2012).
- ⁴⁰A. Gällström, B. Magnusson, S. Leone, O. Kordina, N. T. Son, V. Ivády, A. Gali, I. A. Abrikosov, E. Janzén, and I. G. Ivanov, *Phys. Rev. B* **92**, 075207 (2015).
- ⁴¹N. T. Son, A. Ellison, B. Magnusson, M. F. MacMillan, W. M. Chen, B. Monemar, and E. Janzén, *J. Appl. Phys.* **86**, 4348 (1999).
- ⁴²A. Gällström, B. Magnusson, and E. Janzén, *Mater. Sci. Forum* **615-617**, 405 (2009).
- ⁴³T. Bosma, G. J. J. Lof, C. M. Gilardoni, O. V. Zwier, F. Hendriks, B. Magnusson, A. Ellison, A. Gällström, I. G. Ivanov, N. T. Son, R. W. A. Havenith, and C. H. van der Wal, *npj Quantum Inf.* **4**, 48 (2018).
- ⁴⁴A. Gällström, B. Magnusson, F. C. Beyer, A. Gali, N. T. Son, S. Leone, I. G. Ivanov, C. G. Hemmingsson, A. Henry, and E. Janzén, *Physica B* **407**, 1462 (2012).
- ⁴⁵L. Spindlberger, A. Csóré, G. Thiering, S. Putz, R. Karhu, J. Ul Hassan, N. T. Son, T. Fromherz, A. Gali, and M. Trupke, *Phys. Rev. Appl.* **12**, 014015 (2019).
- ⁴⁶G. Wolfowicz, C. P. Anderson, B. Diler, O. G. Poluektov, F. J. Heremans, and D. D. Awschalom, [arXiv:1908.09817](https://arxiv.org/abs/1908.09817).
- ⁴⁷H. J. von Bardeleben, J. L. Cantin, A. Csóré, A. Gali, E. Rauls, and U. Gerstmann, *Phys. Rev. B* **94**, 121202(R) (2016).
- ⁴⁸S. A. Zargaleh, B. Eble, S. Hameau, J.-L. Cantin, L. Legrand, M. Bernard, F. Margailan, J.-S. Lauret, J.-F. Roch, H. J. von Bardeleben, E. Rauls, U. Gerstmann, and F. Treussart, *Phys. Rev. B* **94**, 060102(R) (2016).
- ⁴⁹W. F. Koehl, B. Diler, S. J. Whiteley, A. Bourassa, N. T. Son, E. Janzén, and D. D. Awschalom, *Phys. Rev. B* **95**, 035207 (2017).
- ⁵⁰B. Diler, S. J. Whiteley, C. P. Anderson, G. Wolfowicz, M. E. Wesson, E. S. Bielejec, F. Joseph Heremans, and D. D. Awschalom, *npj Quantum Inf.* **6**, 11 (2020).
- ⁵¹J.-F. Wang, F.-F. Yan, Q. Li, Z.-H. Liu, H. Liu, G.-P. Guo, L.-P. Guo, X. Zhou, J.-M. Cui, J. Wang, Z.-Q. Zhou, X.-Y. Xu, J. Xu, C.-F. Li, and G.-C. Guo, [arXiv:1909.12481](https://arxiv.org/abs/1909.12481)
- ⁵²Z. Mu, S. A. Zargaleh, H. J. von Bardeleben, J. E. Froch, H. Cai, X. Yang, J. Yang, X. Li, I. Aharonovich, and W. Gao, [arXiv:2002.02613](https://arxiv.org/abs/2002.02613)
- ⁵³P. Udvarhelyi, G. Thiering, N. Morioka, C. Babin, F. Kaiser, D. Lukin, T. Ohshima, J. Ul-Hassan, N. T. Son, J. Vučković, J. Wrachtrup, and A. Gali, [arXiv:2001.02459](https://arxiv.org/abs/2001.02459)
- ⁵⁴N. T. Son, P. Carlsson, J. Ul Hassan, E. Janzén, T. Umeda, J. Isoya, A. Gali, M. Bockstedte, N. Morishita, T. Ohshima, and H. Itoh, *Phys. Rev. Lett.* **96**, 055501 (2006).
- ⁵⁵A. Falk, B. B. Buckley, G. Calusine, W. F. Koehl, V. V. Dobrovitski, A. Politi, C. A. Zorman, P. X.-L. Feng, and D. D. Awschalom, *Nat. Commun.* **4**, 1819 (2013).
- ⁵⁶Ö. O. Soykal, P. Dev, and S. E. Economou, *Phys. Rev. B* **93**, 081207(R) (2016).
- ⁵⁷H. B. Banks, Ö. O. Soykal, R. L. Myers-Ward, D. K. Gaskill, T. L. Reinecke, and S. G. Carter, *Phys. Rev. Appl.* **11**, 024013 (2019).
- ⁵⁸M. Raha, S. Chen, C. Phenicie, S. Ourari, A. M. Dibos, and J. D. Thompson, [arXiv:1907.09992](https://arxiv.org/abs/1907.09992)
- ⁵⁹D. O. Bracher, X. Zhang, and E. L. Hu, *Proc. Natl. Acad. Sci. U. S. A.* **114**, 4060 (2017).
- ⁶⁰D. M. Lukin, C. Dory, M. A. Guidry, K. Y. Yang, S. Deb Mishra, R. Trivedi, M. Radulaski, S. Sun, D. Vercruyse, G. H. Ahn, and J. Vučković, *Nat. Photonics* **14**, 330 (2019).
- ⁶¹A. L. Crook, C. P. Anderson, K. C. Miao, A. Bourassa, H. Lee, S. L. Bayliss, D. O. Bracher, X. Zhang, H. Abe, T. Ohshima, E. L. Hu, and D. D. Awschalom, [arXiv:2003.00042](https://arxiv.org/abs/2003.00042)
- ⁶²B.-S. Song, T. Asano, S. Jeon, H. Kim, C. Chen, D. D. Kang, and S. Noda, *Optica* **6**, 991 (2019).
- ⁶³G. Wolfowicz, C. P. Anderson, A. L. Yeats, S. J. Whiteley, J. Niklas, O. G. Poluektov, F. J. Heremans, and D. D. Awschalom, *Nat. Commun.* **8**, 1876 (2017).
- ⁶⁴B. Magnusson, N. T. Son, A. Csore, A. Gällström, T. Ohshima, A. Gali, and I. G. Ivanov, *Phys. Rev. B* **98**, 195202 (2018).
- ⁶⁵M. Widmann, M. Niethammer, D. Y. Fedyanin, I. A. Khramtsov, I. D. Booker, J. Ul Hassan, S. Lasse, T. Rendler, R. Nagy, N. Morioka, I. G. Ivanov, N. T. Son, T. Ohshima, M. Bockstedte, A. Gali, C. Bonato, S.-Y. Lee, and J. Wrachtrup, *Nano Lett.* **19**, 7173 (2019).
- ⁶⁶M. Rühl, L. Bergmann, M. Krieger, and H. B. Weber, *Nano Lett.* **20**, 658 (2020).
- ⁶⁷N. Morioka, C. Babin, R. Nagy, I. Gediz, E. Hesselmeier, D. Liu, M. Joliffe, M. Niethammer, D. Dasari, V. Vorobyov *et al.*, [arXiv:2001.02455](https://arxiv.org/abs/2001.02455).
- ⁶⁸L. Robledo, L. Childress, H. Bernien, B. Hensen, P. F. A. Alkemade, and R. Hanson, *Nature* **477**, 574 (2011).
- ⁶⁹P. Neumann, J. Beck, M. Steiner, F. Rempp, H. Fedder, P. R. Hemmer, J. Wrachtrup, and F. Jelezko, *Science* **329**, 542 (2010).
- ⁷⁰P. C. Maurer, G. Kucsko, C. Latta, L. Jiang, N. Y. Yao, S. D. Bennett, F. Pastawski, D. Hunger, N. Chisholm, M. Markham, D. J. Twitchen, J. I. Cirac, and M. D. Lukin, *Science* **336**, 1283 (2012).
- ⁷¹A. Dreau, P. Spinicelli, J. R. Maze, J.-F. Roch, and V. Jacques, *Phys. Rev. Lett.* **110**, 060502 (2013).